Electronic Supplementary Material (ESI) for Chemical Communications

Supporting Information

Metal ion binding properties of DNA duplexes containing thiopyrimidine base pairs

Itaru Okamoto, Takashi Ono, Rimi Sameshima, and Akira Ono
Department of Material and Life Chemistry, Faculty of Engineering, Kanagawa University, 3-27-1 Rokkakubashi, Kanagawa-ku, Yokohama 221-8686, Japan. akiraono@kanagawa-u.ac.jp

Synthesis of oligonucleotides

Oligonucleotides containing 2-thiothymidine, 4-thiothymidine and 4-thiouracil bases were synthesized on a 1 μmol scale using an ABI 394 DNA/RNA synthesizer, using commercially available phosphoramidites from Glen Research. Deprotection was performed according to protocols to provided by the vender. All oligonucleotides were purified by reverse–phase HPLC and confirmed by MALDI–TOF MS. HPLC profiles and MALDI-TOF MS spectra of purified oligonucleotides were shown in Figure S1 and Figure S2.

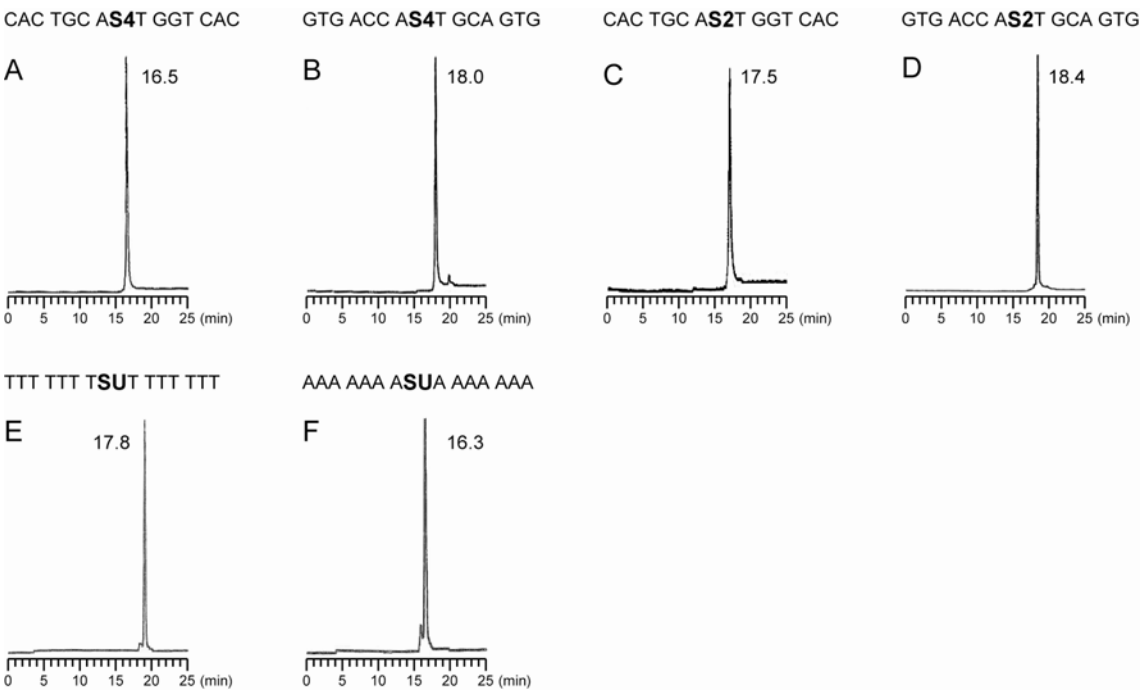

Figure S1 A-F) Reverse–phase HPLC profiles of purified oligonucleotides containing thiopyrimidine bases. A,B) oligonucleotides containing S4 base C,D) oligonucleotides containing S2 base E,F) oligonucleotides containing SU base.

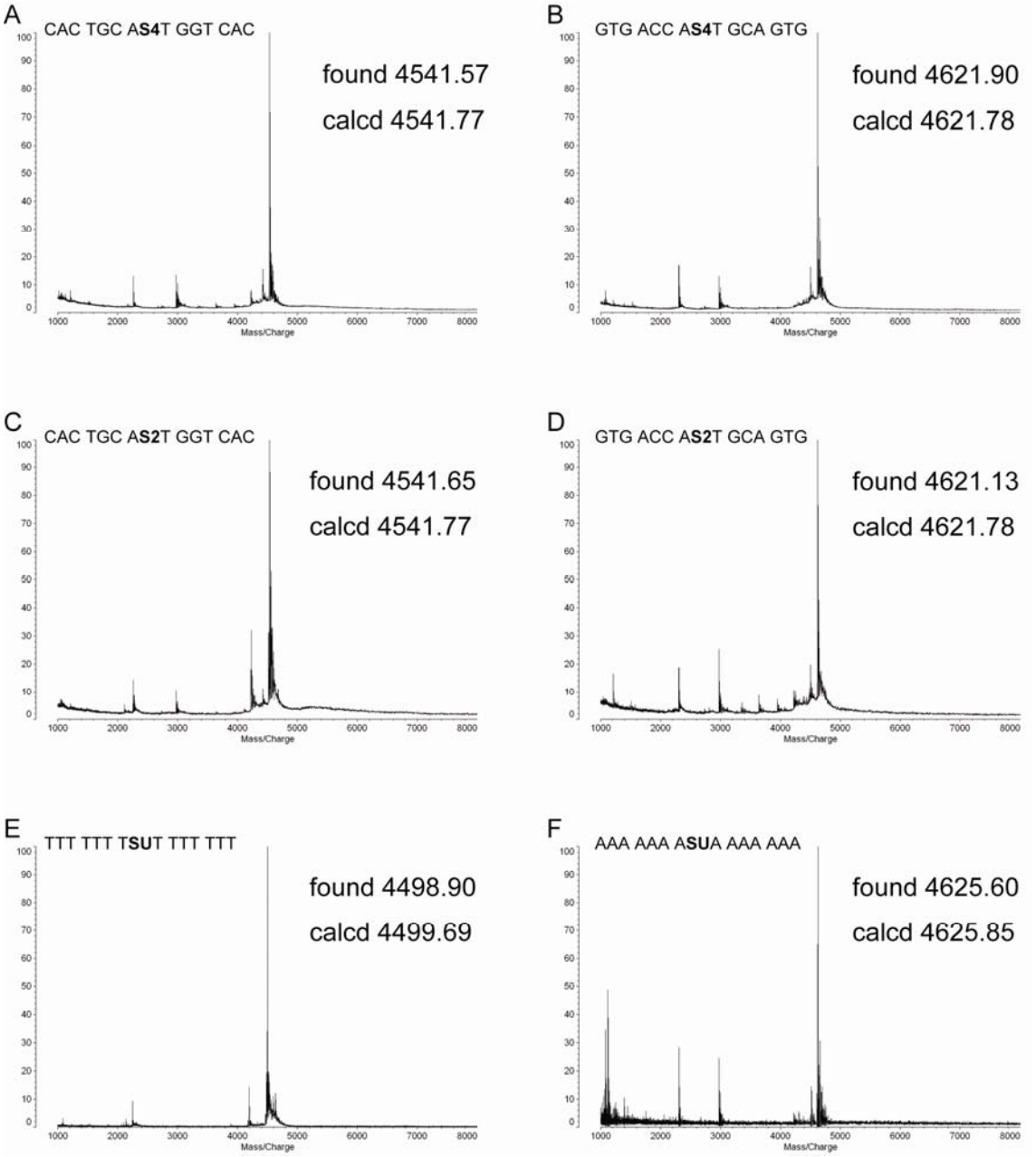

Figure S2 A-F) MALDI–TOF MS spectra of oligonucleotides containing thiopyrimidine bases. A,B) oligonucleotides containing S4 base C,D) oligonucleotides containing S2 base E,F) oligonucleotides containing SU base.

Synthesis of oligonucleotide containing 4S-methylthiourasil base

A solution of 12 mer d(TTT TTT TSUT TTT) (3 O.D.) in a mixture of 0.1 M potassium phosphate buffer (200 μL, pH 8) and DMF (20 μL) was treated with excess methyl iodide (1 μL). After three hours at room temperature, the reaction mixture was extracted with ether (3 × 1 mL), and traces of ether in the aqueous phase were removed using a gentle stream of Ar (5 min). The aqueous solution was passed through a 0.2 μm membrane filter, and S-methylated oligonucleotide was analyzed and purified by reverse–phase HPLC. HPLC profiles of non-methylated and S-methylated oligonucleotides were shown in Figure S3A and S3B. Although, the retention times of these oligonucleotides were very close, slightly divided two peaks were observed in Figure S3C (analysis of sample containing both non-methylaed and S-methylated oligonulcoeitdes). The structure of S-methylated oligonucleotide was confirmed by MALDI-TOF MS (Figure S3D).

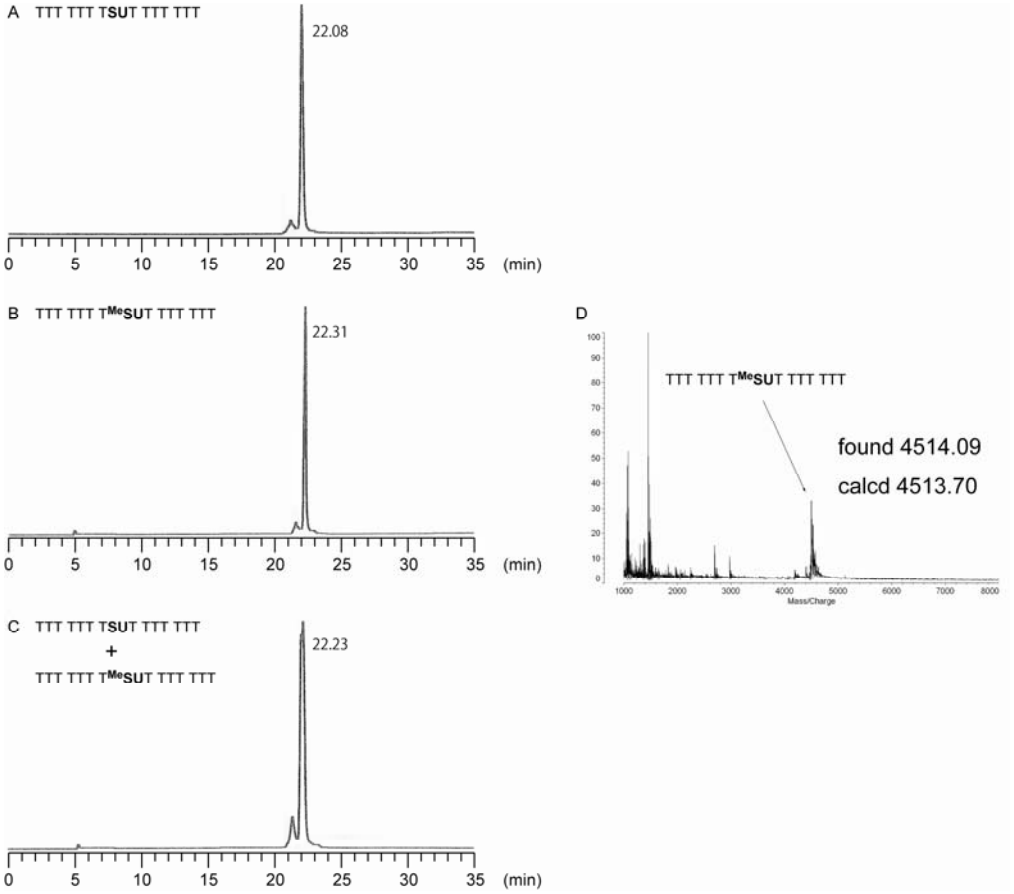

Figure S3 A-C) Reverse–phase HPLC profiles. (A) before methylation reaction (B) after methylation reaction (C) analysis of sample containing both non-methylated and S-methylated oligonulcoeitdes. D) MALDI-TOF MS spectrum of S-methylated oligonucleotide.

Preparation of samples for thermal denaturation

Oligonucleotides with or without metals were dissolved in appropriate buffer solutions and heated at 90 °C in a hot water bath for 10 min. The bath temperature was gradually decreased to room temperature and kept at this temperature for 1 h before thermal denaturation.

General method for electrospray ionization mass spectroscopy

ESI–MS measurements were performed on a time–of–flight mass spectrometer (JMS–T100; JEOL, Tokyo, Japan). The measurement conditions were as follows: needle voltage –1.5 kV; orifice voltage –50 V; desolvation temperature 80–100 °C; resolution (10% valley definition) 4000; and sample flow rate 20 μL min^{-1}. For sample preparation, each aqueous solution containing DNA and metal ions in 62.5 mM NH_4OAc (pH 7) was diluted with MeOH. The DNA concentration was 10 μM, the buffer (NH_4OAc) concentration was 50 mM, and the solvent was H_2O/MeOH (4:1).

Thermal denaturation profiles of the duplex-S2 and duplex-S4 in solutions containing various concentrations of Hg(II) ions (0 to 3.0 equivalents).

Both duplexes were stabilized by addition of Hg(II) ions, although stabilizing effects of the metal ion were different with duplexes (Fig. S4a and c). **Duplex-S4** was largely stabilized in the presence of 1 equivalent of Hg(II) ions (ΔT_m = 20 °C), whereas stabilizing effect of the metal ions on **duplex-S2** was smaller (ΔT_m = 10 °C). We do not have proper explanations for the difference.

In the presence of less than one equivalent of Hg(II) ions, two transition curves were observed in each denaturation profiles for both duplexes (Fig. S4a and c), which may indicate that Hg(II) ions, once captured between thiopyrimidine bases, dissociate slowly and stand between bases at least in time scale of denaturation process. By addition of more than one equivalent of Hg(II) ions, both duplexes started to denaturate at temperatures lower than those in the presence of one equivalent of the metal ions (Fig. S4b and d). Consequently, both **duplex-S2** and **duplex-S4** were fully stabilized in the presence of one equivalent of Hg(II) ions, whereas addition of the excess of the metal ions destabilized the duplexes.

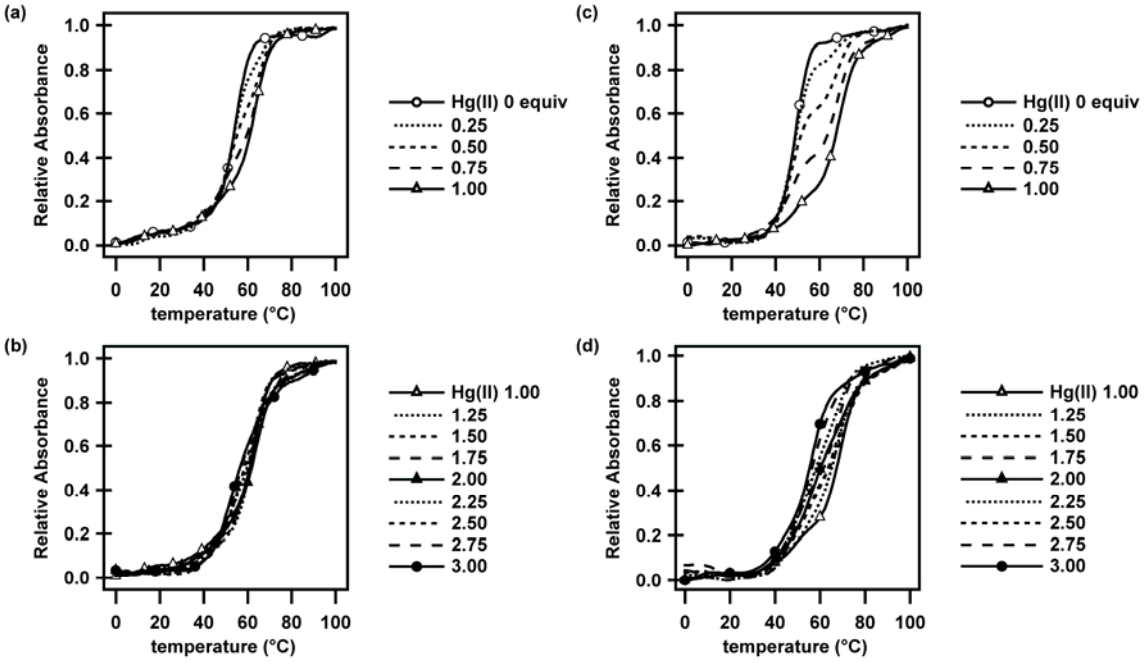

Figure S4 a) duplex-S2 with Hg(II) (0 to 1.0 equivalents); b) duplex-S2 with Hg(II) (1.0 to 3.0 equivalents); c) duplex-S4 with Hg(II) (0 to 1.0 equivalents); d) duplex-S4 with Hg(II) (1.0 to 3.0 equivalents)

ESI–TOF MS spectra of DNA duplexes containing thiopyrimidine base pairs in the presence of Hg(II) ions

In the presence of Hg(II) ions, peaks due to a complex consisting one Hg(II) ion and a duplex were observed (Fig. S5b and d).

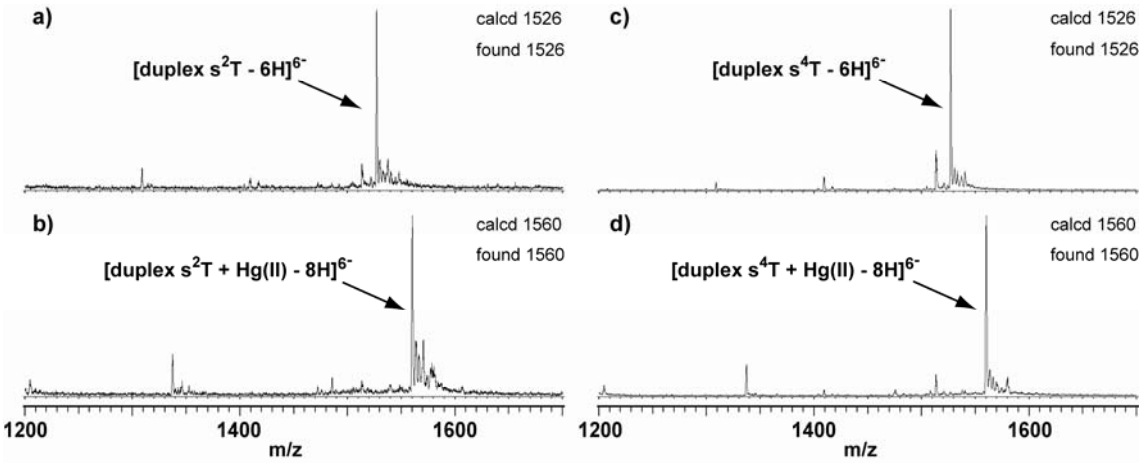

Figure S5 (a) **duplex-S2** and (b) **duplex-S2** in the presence of 2 equiv. of Hg(II) ions, (c) **duplex-S4** and (d) **duplex-S4** in the presence of 2 equiv. of Hg(II) ions.

ESI-TOF MS spectra of duplex-S2

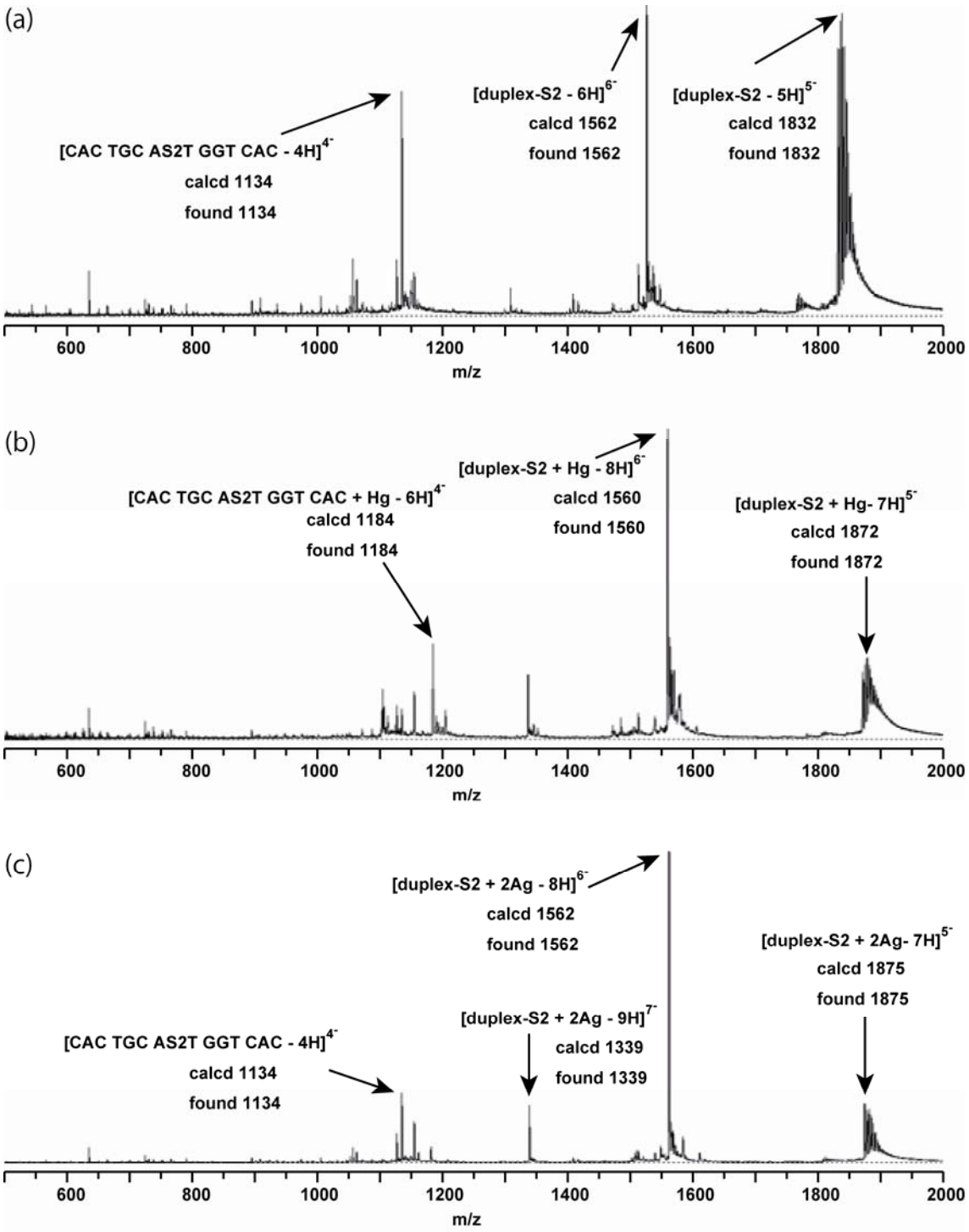

Figure S6 (a) **duplex-S2** in the absence of metal ion. (b) **duplex-S2** in the presence of 2 equiv. of Hg(II) ions. (c) **duplex-S2** in the presence of 2 equiv. of Ag(I) ions.

ESI-TOF MS spectra of duplex-S4

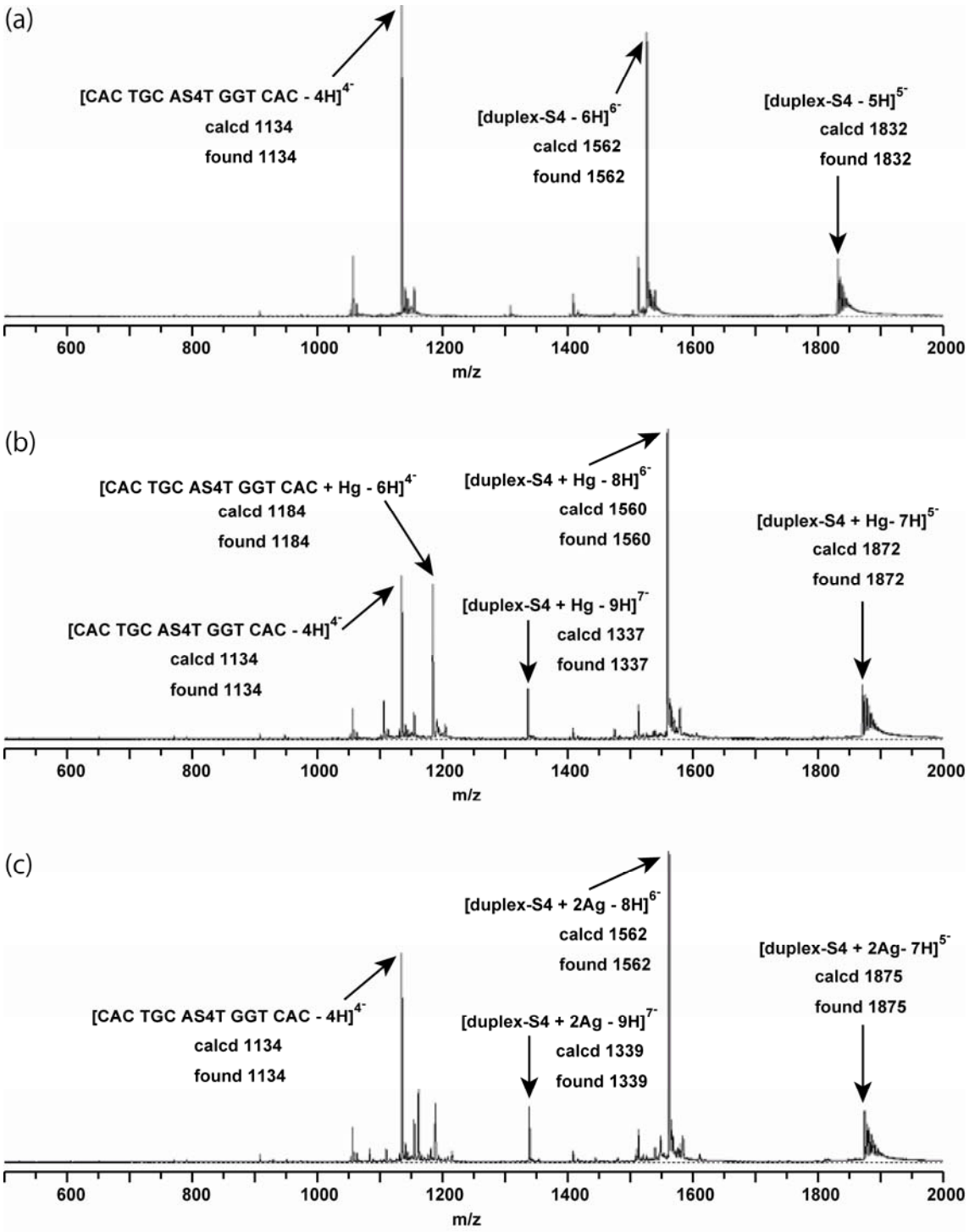

Figure S7 (a) **duplex-S4** in the absence of metal ion. (b) **duplex-S4** in the presence of 2 equiv. of Hg(II) ions. (c) **duplex-S4** in the presence of 2 equiv. of Ag(I) ions.

Thermal denaturation experiments of duplex-S2 and duplex-S4 in the presence of divalent metal ions

It was reported that unpaired thiopyrimidine bases form complexes with divalent metal ions.[1,2] Consequently, it was expected that thermal denaturation profiles of duplexes were changed in the presence of divalent metal ions. However, thermal denaturation profiles did not significantly change in the presence of Mg(II), Ca(II), Fe(II), Co(II), Ni(II), Zn(II), Pd(II), Cd(II), and Pt(II) ions (Figures S8 and S9). These results suggested that the metal ion binding properties of thiopyrimidine base pairs are different from those of unpaired bases. Although a possibility of that the heavy metal ions and the thiopyrimidine pairs form some complexes which, however, did not stabilized the duplex formations.

Thermally induced transition profiles of duplex-S2 in the presence of metal ions.

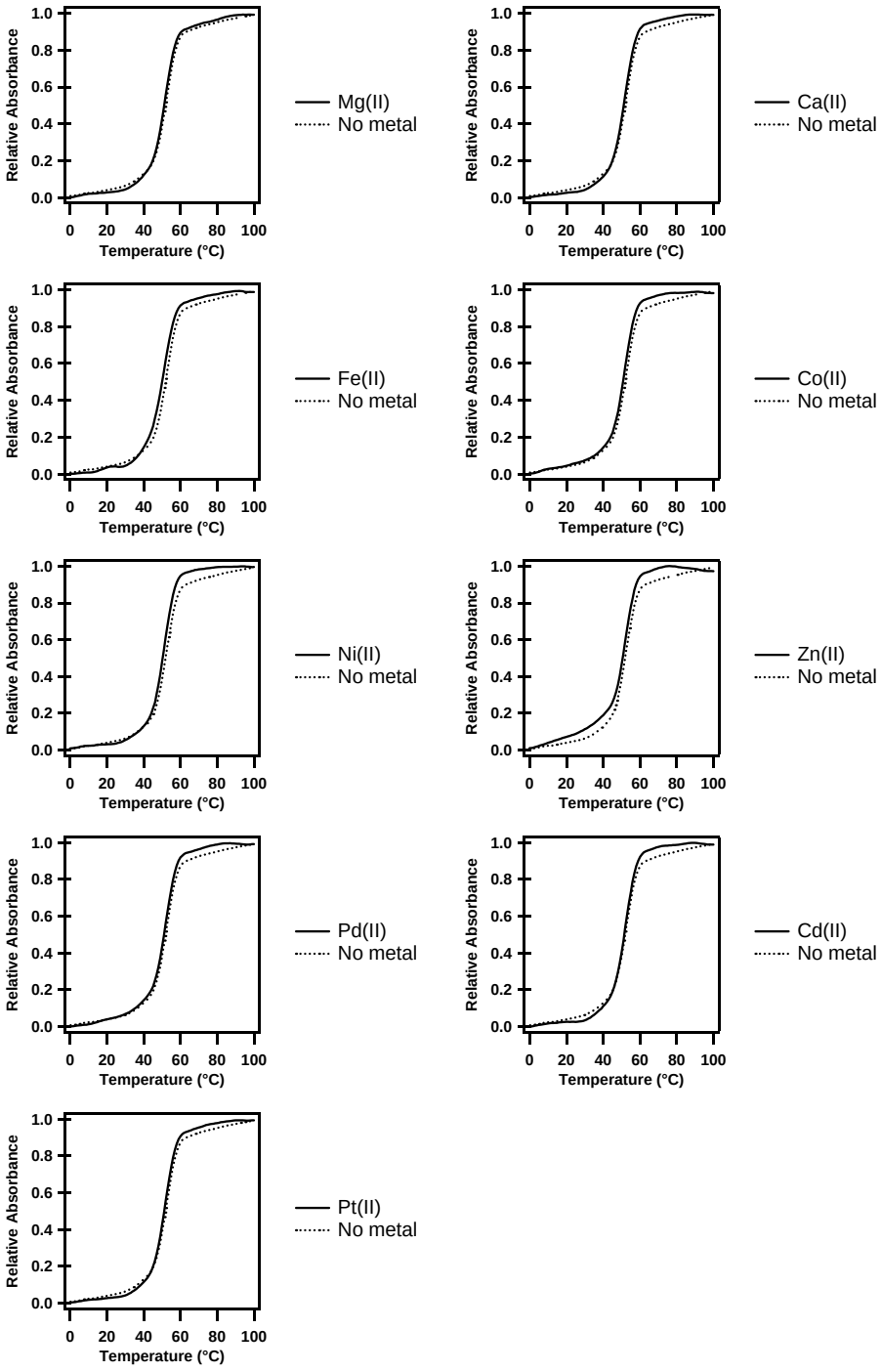

Figure S8 Thermally induced transition profiles of **duplex-S2** in the presence of metal ions. Each solution contained 2 μM duplex, 10 mM MOPS buffer (pH 7), 2 μM metal ions and 100 mM $NaNO_3$.

Thermally induced transition profiles of duplex-S4 in the presence of metal ions.

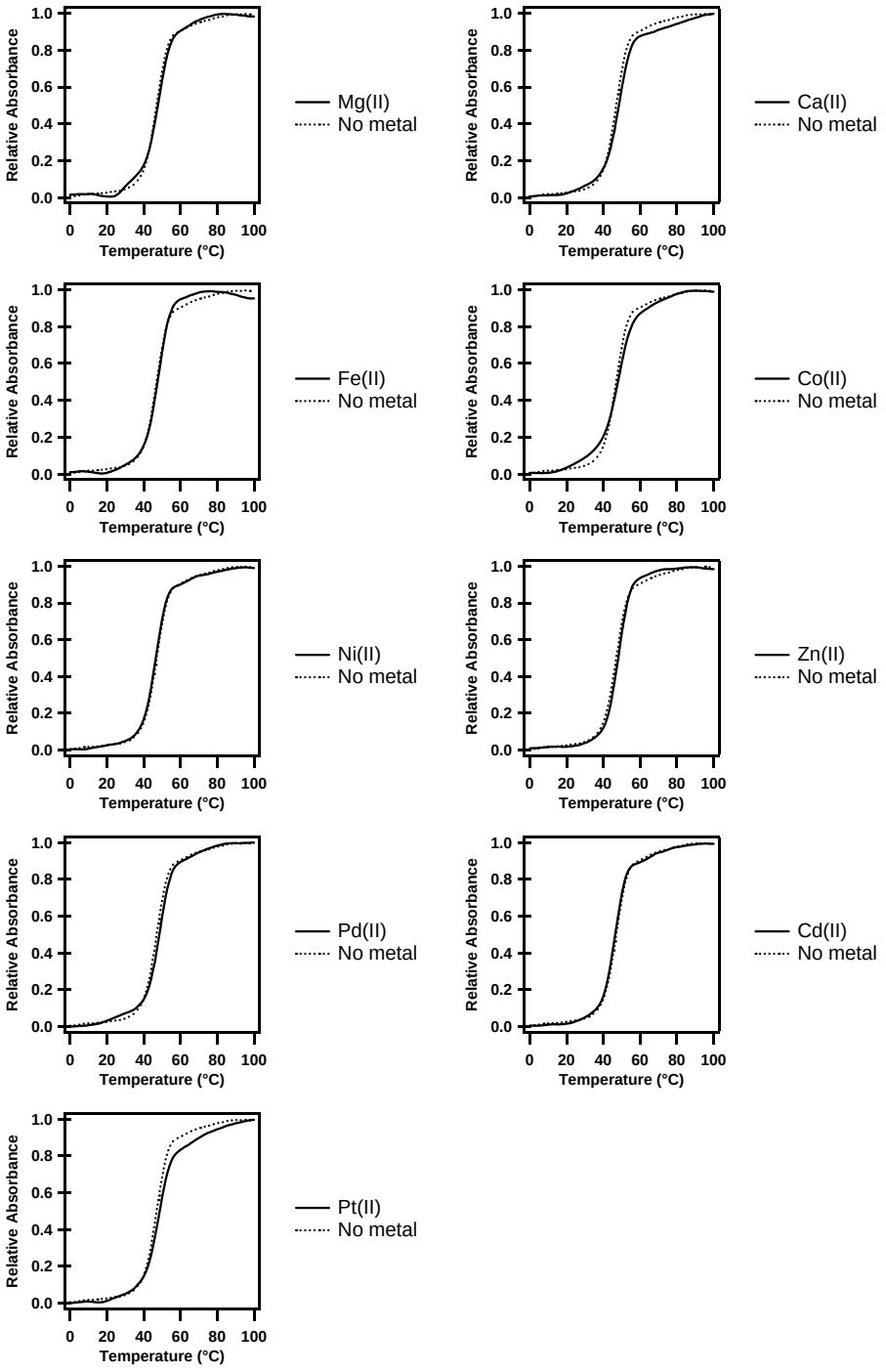

Figure S9 Thermally induced transition profiles of **duplex-S4** in the presence of metal ions. Each solution contained 2 μM duplex, 10 mM MOPS buffer (pH 7), 2 μM metal ions and 100 mM $NaNO_3$.

Thermally induced transition profiles and ESI-TOF MS spectrum of duplex-S2 and duplex-S4 in the presence of Cu(II) ions.

By addition of Cu(II) ions, melting profiles of **duplex-S2** were not remarkably changed (Figure S10A). On the other hand, by addition of Cu(II) ions, transition curves of **duplex-S4** were shifted to higher temperature ranges (Figure S10B). When less than one equivalent of Cu(II) ions were present relative to the S4-S4 base pair, a single transition was observed (Figure S10C). As the concentration of Cu(II) ions increased over one equivalent, thermally induced transitions shifted to higher temperature range and the shapes of these denaturation profiles changed into gradual two transitions (Figure S10D). In ESI-TOF MS analysis, a peak corresponding to complex of **duplex-S4** with two equivalents of Cu(II) ion was observed (Figure S10E). At present, we do not have any experimental evidences indicating a binding scheme of S4-S4 pair and Cu(II) ions.

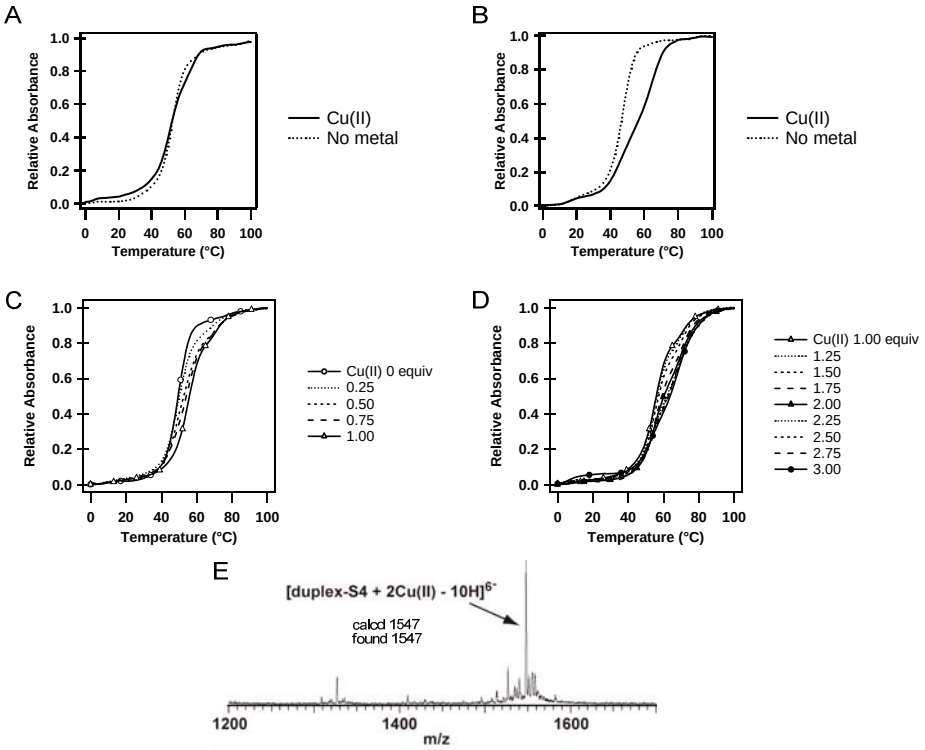

Figure S10 A) Thermally induced transition profiles in a solution containing 2 μM **duplex-S2**, 10 mM MOPS buffer (pH 7), 4 μM Cu(II) ions and 100 mM $NaNO_3$. B-D) Thermally induced transition profiles in a solution containing 2 μM **duplex-S4**, 10 mM MOPS buffer (pH 7), 0.5–6 μM Cu(II) ions and 100 mM $NaNO_3$. (B) 4 μM Cu(II) ions (C) 0.25-2 μM Cu(II) ions (D) 2-6 μM Cu(II) ions. E) ESI-TOF MS spectrum of duplex-S4 with two equivalents of Cu(II) ions.

Thermally induced transition profile and ESI-TOF MS spectrum of duplex-S4 in the presence of Cd(II) ions at pH 9.

In basic solution, **duplex-S4** was slightly stabilized (ΔT_m = 4 °C) in the presence of Cd(II) ions (Figure S11A). In ESI-TOF MS analysis, a peak corresponding to complex of **duplex-S4** with one Cd(II) ion was observed (Figure S11B).

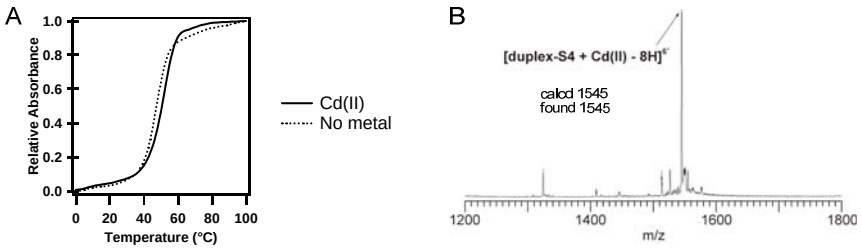

Figure S11 A) Thermally induced transition profiles in a solution containing 2 μM duplex-S4, 10 mM sodium borate buffer (pH 9), 2.2 μM Cd(II) ions and 100 mM $NaNO_3$. B) ESI-TOF MS spectrum of **duplex-S4** with two equivalents of Cd(II) ions: measurement was carried out in a buffer containing 50 mM NH_4OAc (pH 9) and MeOH (H_2O/MeOH = 4:1, v/v).

CD spectra of duplex-S2 on addition of Ag(I) ions (0 to 4.0 equivalents).

In the presence of Ag(I) ions, the CD spectra of **duplex-S2** showed remarkable changes (Figure S12a,b). Generally, 2-thiouridine derivatives have negative bands at around 320–330 nm.[3,4] Thus, the negative band at around 320 nm may be due to the 2'-deoxy-2-thiouridine residues. By adding Ag(I) ions, the negative band at around 320 nm decreased gradually, and the negative band at around 300 nm gradually appeared. In addition, the positive band at around 270 nm gradually decreased. When two equivalents of Ag(I) ions were added, the band at around 320 nm almost disappeared (Figure S12c, open circles) and the ellipticity change at around 300 nm reached a plateau (Figure S12c, closed circles). These negative band changes suggested that two equivalents of Ag(I) ions interacted with the S2–S2 base pairs.

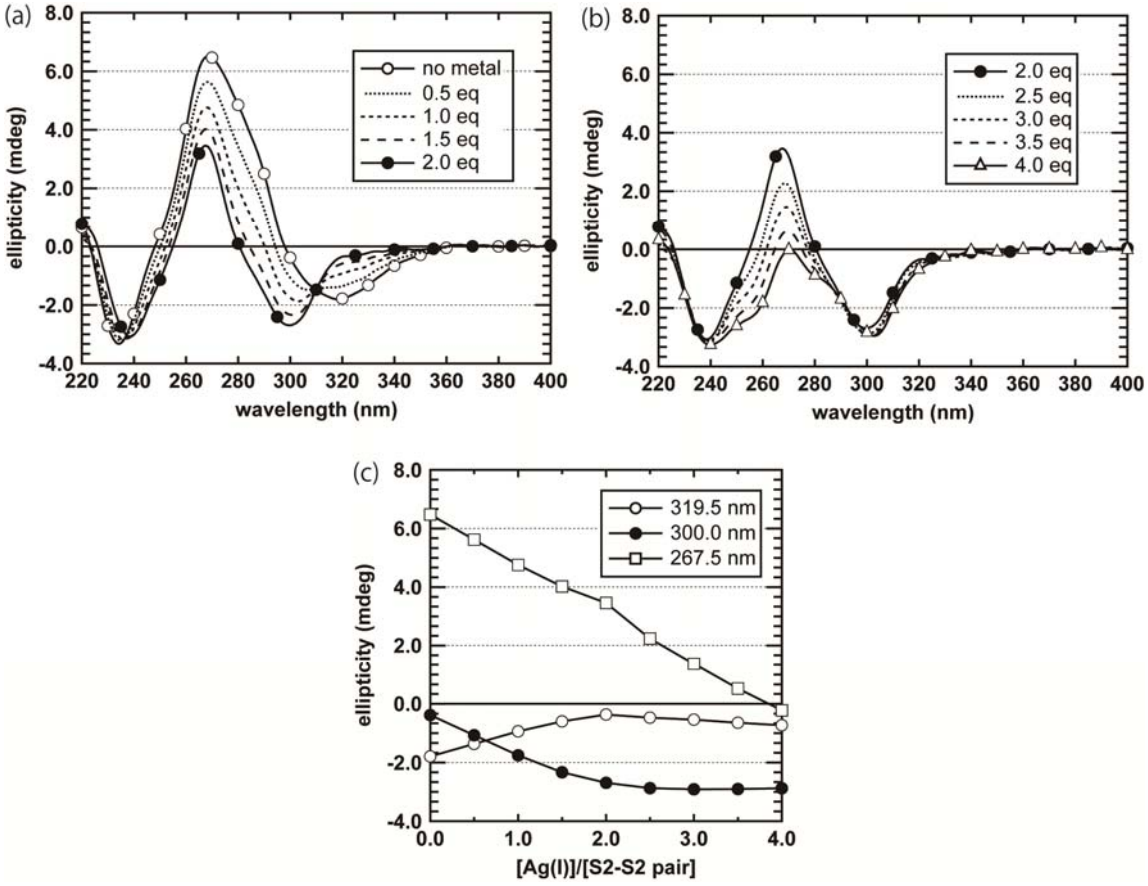

Figure S12 a) duplex-S2 with Ag(I) (0 to 2.0 equivalents); b) duplex-S2 with Ag(I) (2.0 to 4.0 equivalents); c) Ellipticity versus Ag(I) ion concentration. Each solution contained 2 μM duplex in 10 mM Mops, 100 mM $NaClO_4$, pH 7. Each spectrum was measured at 20 °C.

CD spectra of duplex-S4 on addition of Ag(I) ions (0 to 4.0 equivalents).

In the presence of Ag(I) ions, CD spectra of duplex-S4 showed remarkable changes (Figure S13a,b). Based on previous reports, 4-thiouridine derivatives have one negative band at around 360 nm and one positive band at around 325 nm.[5–9] Thus, the negative Cotton effect at around 360 nm and the positive Cotton effect at around 325 nm may be due to 2'-deoxy-4-thiouridine residues. By adding Ag(I) ions, the intensities of the negative band at around 357 nm and of the positive band at around 325 nm gradually increased (Figure S13a). In addition, the intensity of the positive band at around 276 nm also gradually increased. When two equivalents of Ag(I) ions were added, the ellipticity changes at around 357 nm (Figure S13c, open circles) and 325 nm (Figure S13c, closed circles) reached plateaus. These changes suggested that two equivalents of Ag(I) ions interacted with the S4–S4 base pairs.

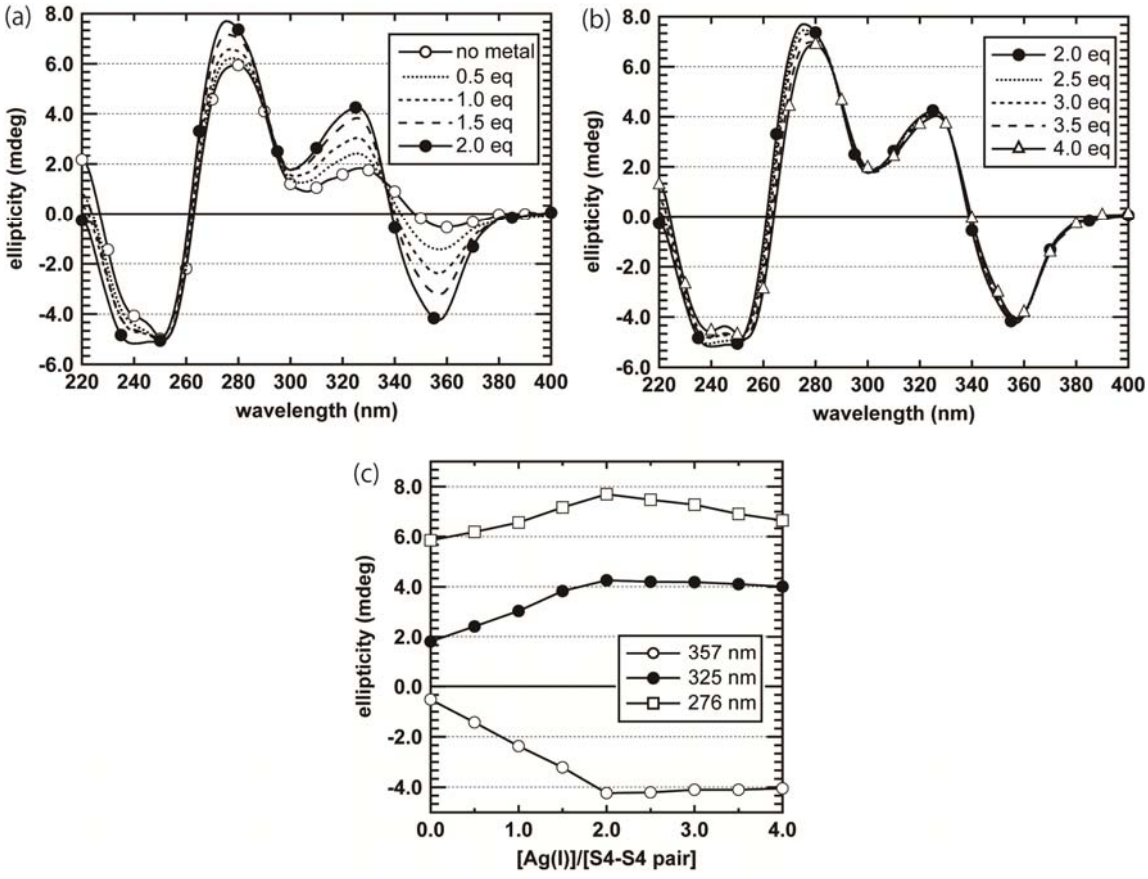

Figure S13 a) duplex-S4 with Ag(I) (0 to 2.0 equivalents); b) duplex-S4 with Ag(I) (2.0 to 4.0 equivalents); c) Ellipticity versus Ag(I) ion concentration. Each solution contained 2 μM duplex in 10 mM Mops, 100 mM $NaClO_4$, pH 7. Each spectrum was measured at 20 °C.

References

1. (a) T. Kowalik-Jankowska, H. Kozlowski, I. Sovago, B. Nawrot, E. Sochacka and A. J. Malkiewicz, *J. Inorg. Biochem.*, 1994, **53**, 49-56. (b) T. Kowalik-Jankowska, K. Varnagy, J. Swiatek-Koztowska, A. Jon, I. Sovago, E. Sochacka, A. Malkiewicz, J. Spychata and H. Koztowski, *J. Inorg. Biochem.*, 1997, **65**, 257-262. (c) J. Swiatek-Kozlowska, J. Brasun, A. Dobosz, E. Sochacka and A. Glowacka, *J. Inorg. Biochem.*, 2003, **93**, 119-124. (d) A. Odani, H. Kozlowski, J. Swiatek-Kozlowska, J. Brasun, B. P. Operschall and H. Sigel, *J. Inorg. Biochem.*, 2007, **101**, 727-735. (e) J. Brasuń, A. Matera, E. Sochacka, J. Swiatek-Kozlowska, H. Kozlowski, B. Operschall and H. Sigel, *J. Biol. Inorg. Chem.*, 2008, **13**, 663-674.
2. O. Iranzo, H. Khalili, D. Epstein and J. Morrow, *J. Biol. Inorg. Chem.*, 2004, **9**, 462-470.
3. T. Ueda and H. Nishino, *Chem. Pharm. Bull.*, 1969, **17**, 920-926.
4. W. Bähr, P. Waerber and K. H. Scheit., *Eur. J. Biochem.*, 1973, **33**, 535-544.
5. J. F. Scott and P. Schofield, *Proc. Nat. Acad. Sci. USA*, 1969, **64**, 931-938.
6. G. E. Willick and C. M. Kay, *Biochemistry*, 1971, **10**, 2216-2222.
7. K. Watanabe and K. Imabori, *Biochem. Biophys. Res. Commun.*, 1971, **45**, 488-494.
8. M. Saneyoshi, T. Anami, S. Nishimura and T. Samejima, *Arch. Biochem. Biophys.*, 1972, **152**, 677-684.
9. G. E. Willick, K. Oikawa and C. M. Kay, *Biochemistry*, 1973, **12**, 899-904.